

RESEARCH ARTICLE

A mathematical model analyzing temperature threshold dependence in cold sensitive neurons

Kees McGahan¹*, James Keener²

Department of Mathematics, University of Utah, Salt Lake City, Utah, United States of America

* These authors contributed equally to this work.

* mcgahan@math.utah.edu

Abstract

Here we examine a class of neurons that have been recently explored, the somatosensory neuronal subclass of cold thermosensors. We create a mathematical model of a cold sensing neuron that has been formulated to understand the variety of ionic channels involved. In particular this model showcases the role of TRPM8 and voltage gated potassium channels in setting the temperature dependent activation and inactivation threshold level. Bifurcation analysis of the model demonstrates that a Hodgkin-Huxley type model with additional TRPM8 channels is sufficient to replicate observable experimental features of when different threshold level cold thermosensors turn on. Additionally, our analysis gives insight into what is happening at the temperature levels at which these neurons shut off and the role sodium and leak currents may have in this. This type of model construction and analysis provides a framework moving forward that will help tackle less well understood neuronal classes and their important ionic channels.

OPEN ACCESS

Citation: McGahan K, Keener J (2020) A mathematical model analyzing temperature threshold dependence in cold sensitive neurons. PLoS ONE 15(8): e0237347. <https://doi.org/10.1371/journal.pone.0237347>

Editor: David D McKerny, University of Southern California, UNITED STATES

Received: April 9, 2020

Accepted: July 23, 2020

Published: August 12, 2020

Peer Review History: PLOS recognizes the benefits of transparency in the peer review process; therefore, we enable the publication of all of the content of peer review and author responses alongside final, published articles. The editorial history of this article is available here: <https://doi.org/10.1371/journal.pone.0237347>

Copyright: © 2020 McGahan, Keener. This is an open access article distributed under the terms of the [Creative Commons Attribution License](https://creativecommons.org/licenses/by/4.0/), which permits unrestricted use, distribution, and reproduction in any medium, provided the original author and source are credited.

Data Availability Statement: The data (code) underlying the results presented in the study are available from <https://github.com/keesmccgahan/TRPM8-Model>.

Introduction

With the progress being made in genomics and molecular genetics recently there has never been a better time to explore the nervous system and its disorders. One approach to investigating the nervous system is to focus on individual neurons and determine their contribution to the entire complex. The key to this approach is creating a functional profile of the neurons and breaking them into categories or classes. This technique revolves around either identifying the types of compounds that activate the neuron, or the types of receptors and ionic channels on the cell's surface [1].

One such classification technique is constellation pharmacology, a technique which was recently utilized to further the understanding of cold thermosensors [2]. These dorsal root and trigeminal ganglion neurons are characterized by responsiveness to ATP, menthol, mustard oil, and a varying range of cold temperatures. This varying range of temperature activation has led to describing the receptiveness of these neurons to temperature as either high or low

Funding: The author(s) received no specific funding for this work.

Competing interests: The authors have declared that no competing interests exist.

threshold. The low threshold cold responsive neurons are typically described to activate between 20°C and 30°C while the high threshold neurons respond to temperatures between 8°C and 20°C [2–5]. These threshold levels have been used to divide cold responsive neurons into two classes: cool thermoreceptors and cold nociceptors [3, 6].

The process of discovering the ion channels that categorize these cold thermosensors has also begun to shed light on this temperature threshold difference. One critical defining feature of these cold sensors was found to be the presence of TRPM8, a channel from the transient receptor potential superfamily [5, 7]. These channels are voltage gated with their open probability influenced by multiple things, but primarily temperature. While TRPM8 has been marked as a critical channel in defining cold responsive neurons, TRPA1 and *Na_v1.8*, a cold insensitive sodium channel, are believed to play roles at extreme low temperatures [5, 6]. In addition to these cold specific ion channels, voltage gated potassium channels have also been hypothesized to influence the temperature threshold level of activation [2, 8]. In particular, it is thought that the ratio of TRPM8 channel to *K_v1* potassium channel density controls the threshold level. It has been shown that blocking TRPM8 channels can force a neuron to switch to a higher threshold and then applying an additional blocker of *K_v1* channels can restore the neuron to its initial threshold level [8].

Although a multitude of labs have experimentally examined cold sensing neurons, few attempts have been made to model their behavior mathematically. The first main attempts were of the Huber-Braun cold receptor variety which showed the desired response to temperature, but did not include TRPM8 channel activity or the ability to track sodium and potassium ion fluxes [9]. With the discovery of the importance of TRPM8 channels, models were created and parameters experimentally fit for TRPM8 channels and their activation curves [7]. These models include a version without menthol and two versions with menthol; the Hodgkin-Huxley version and the Monod-Wyman-Changeux type model. The development of a mathematical model of the TRPM8 channel allowed for including this new channel into a modified version of the Huber-Braun model [10]. Although successfully highlighting the importance of TRPM8 in creating a cold thermosensor, this model focuses only on cold sensitive neurons activating above 20°C and leaves out exploring what sets the temperature threshold level for activation and the corresponding role of potassium channels [10].

Here we develop a biologically driven model of a general cold thermosensor that includes the presence of TRPM8 channels. The foundation of this model is the Hodgkin-Huxley model from 1952 with the secondary component being the addition of the TRPM8 model without menthol from the Voets lab [11, 12]. The goals of our model are as follows:

1. to explicitly track differences in temperature dependent response in cold sensitive neurons as it relates to having different ion channel densities
2. to examine how specifically tuned high and low threshold cold sensitive neurons can be with regards to their activating and inactivating temperatures
3. to showcase the ability of simple physiological models to examine biological features and questions in neuroscience that have proven difficult to examine experimentally.

Materials and methods

The model is composed of a general Hodgkin-Huxley neuron with an additional current through the TRPM8 channel [12]. All combined, this gives the following for membrane voltage

V with gating variables m, n, h :

$$\frac{dV}{dt} = \frac{1}{Cm} (-I_{Na} - I_K - I_l - I_{m8}) \quad (1)$$

$$\frac{dj}{dt} = \Phi(T)[a_j(V)(1-j) - b_j(V)j]; j = m, n, h \quad (2)$$

The Hodgkin-Huxley current equations have the form:

$$I_{Na} = g_{Na} m^3 h (V - E_{Na}) \quad (3)$$

$$I_K = g_K n^4 (V - E_K) \quad (4)$$

$$I_l = g_l (V - E_l) \quad (5)$$

where I_K is the potassium current, I_{Na} the sodium current and I_l the leak current. The additional parameters include the equilibrium potentials of the various ions E_{Na} , E_K , E_l , the maximum ionic conductances g_{Na} , g_K , g_l and the membrane capacitance C_m . Finally, the rate constants a_j and b_j were experimentally fitted to exponential functions to give the 6 equations below:

$$a_m(V) = \frac{0.1(V_r - V + 25)}{\exp\left(\frac{V_r - V + 25}{10}\right) - 1} \quad (6)$$

$$B_m(V) = 4 \exp\left(\frac{V_r - V}{18}\right) \quad (7)$$

$$a_h(V) = 0.07 \exp\left(\frac{V_r - V}{20}\right) \quad (8)$$

$$B_h(V) = \frac{1}{\exp\left(\frac{V_r - V + 30}{10}\right) + 1} \quad (9)$$

$$a_n(V) = \frac{0.01(V_r - V + 10)}{\exp\left(\frac{V_r - V + 10}{10}\right) - 1} \quad (10)$$

$$B_n(V) = 0.125 \exp\left(\frac{V_r - V}{80}\right). \quad (11)$$

The final portion of the Hodgkin-Huxley parameters and equations are V_r which represents the equilibrium resting potential and $\Phi(T)$ which is a temperature dependent coefficient that adjusts the rate constants from having been experimentally calculated at 6.3°C. The values of all Hodgkin-Huxley parameters are $V_r = -65\text{mV}$, $E_{Na} = V_r + 115\text{mV}$, $E_K = V_r - 12\text{mV}$, $E_l = V_r + 10.613\text{mV}$, $\Phi(T) = 3^{\frac{T-6.3}{10}}$, $g_{Na} = 120\text{mS/cm}^2$, $g_K = 36\text{mS/cm}^2$, $g_l = 0.3\text{mS/cm}^2$, $C_m = 1\mu\text{F/cm}^2$. In addition to the Hodgkin-Huxley base model, we include a current for the cold sensing TRPM8 channel. We give the current the basic form:

$$I_{m8} = g_{m8} a_{m8} (V - E_{m8}) \quad (12)$$

where, as before, g_{m8} is the maximal conductance of TRPM8 and E_{m8} the reversal potential for TRPM8 channels. From the Voets lab we have the open probability of the channel, a_{m8} , is temperature dependent and given by

$$a_{m8} = \frac{1}{1 + \exp\left(\frac{\Delta H - (T+273.15)\Delta S - zFV/1000}{R(T+273.15)}\right)}, \quad (13)$$

where ΔH and ΔS are the difference in enthalpy and entropy between the open and closed states, z is the gating charge, F and R are Faraday's and the universal gas constant, and T is temperature in degrees Celsius [7, 11]. With R and F being assigned their classical value, the remainder of the TRPM8 channel parameters were experimentally fit to yield $\Delta H = -156 \frac{\text{kJ}}{\text{mol}}$, $\Delta S = -550 \frac{\text{J}}{\text{molK}}$, $z = 0.87$, $R = 8.3144 \frac{\text{J}}{\text{molK}}$, $F = 96485 \frac{\text{C}}{\text{mol}}$. Note that the parameters to vary are the maximal conductance of the various ion channels, g_{m8} , g_K , g_I and g_{Na} and temperature T . These allow us to examine the neuron's response to temperature and how the relative densities of the ion channels present effect at which temperature level the neurons activate and inactivate. The reversal potential of the TRPM8 channels, E_{m8} has been experimentally shown to be near 0mV and hence for all analysis we set $E_{m8} = 0$ [13].

All bifurcation analysis is done using the software XPPAUT [14]. The temperature ramp and fixed temperature simulations are run in MATLAB [15].

Results

Before analyzing the full model, it is important to see how temperature affects the basic Hodgkin-Huxley model ($g_{m8} = 0$). We begin by looking at the temperature and maximal potassium conductance g_K two parameter bifurcation diagram (Fig 1). Under the Hodgkin-Huxley model structure there are two types of stable, and hence observable, solutions. There is a stable steady state solution which occurs at the resting membrane potential and a stable periodic solution which is periodic action potential spiking. Note, the bifurcation diagrams presented in this analysis show separations of parameter space into regions with different solutions types.

This parameter space is broken up into 3 regions by two curves. Region I corresponds to the parameter values that have no oscillatory solutions with only a stable steady state solution for the voltage variable V . In region II, sandwiched between the blue and black curves, we have the parameter values for which there exists both stable and unstable oscillatory solutions in addition to a stable steady state solution. In this region, the neuron's behavior (oscillatory or steady state) is dependent upon the given initial data. Finally, region III, the area bordered by the blue curve, has stable oscillatory solution coexisting with an unstable steady state solution. The curves are indicating the bifurcations that are occurring in parameter space. The black curve is representative of a saddle-node-periodic bifurcation (SNP) that corresponds to the creation of the two (one stable and one unstable) periodic solutions. Additionally, the blue curve is the Hopf bifurcation that corresponds to the transition to a stable oscillatory solution and unstable steady state. The final regions of interest are the meeting points between the SNP (black) and Hopf (blue) curves which are codimension 2 bifurcation points.

Analysis can be done on these bifurcation plots by fixing one parameter at specific values and then observing the dynamics of V as the other parameter changes. Starting at the standard Hodgkin-Huxley parameter values namely, $g_K = 36$, the neuron has a stable steady state for all temperature values which is seen by noting that the neuron is in region I. Consider a vertical slice with temperature set to 15°C and $g_K = 36$. As g_K is decreased, the neuron crosses the black (SNP) curve in Fig 1 from region I to II, corresponding to the appearance of two oscillatory solutions, one unstable and one stable. Then continuing to decrease g_K leads the neuron to

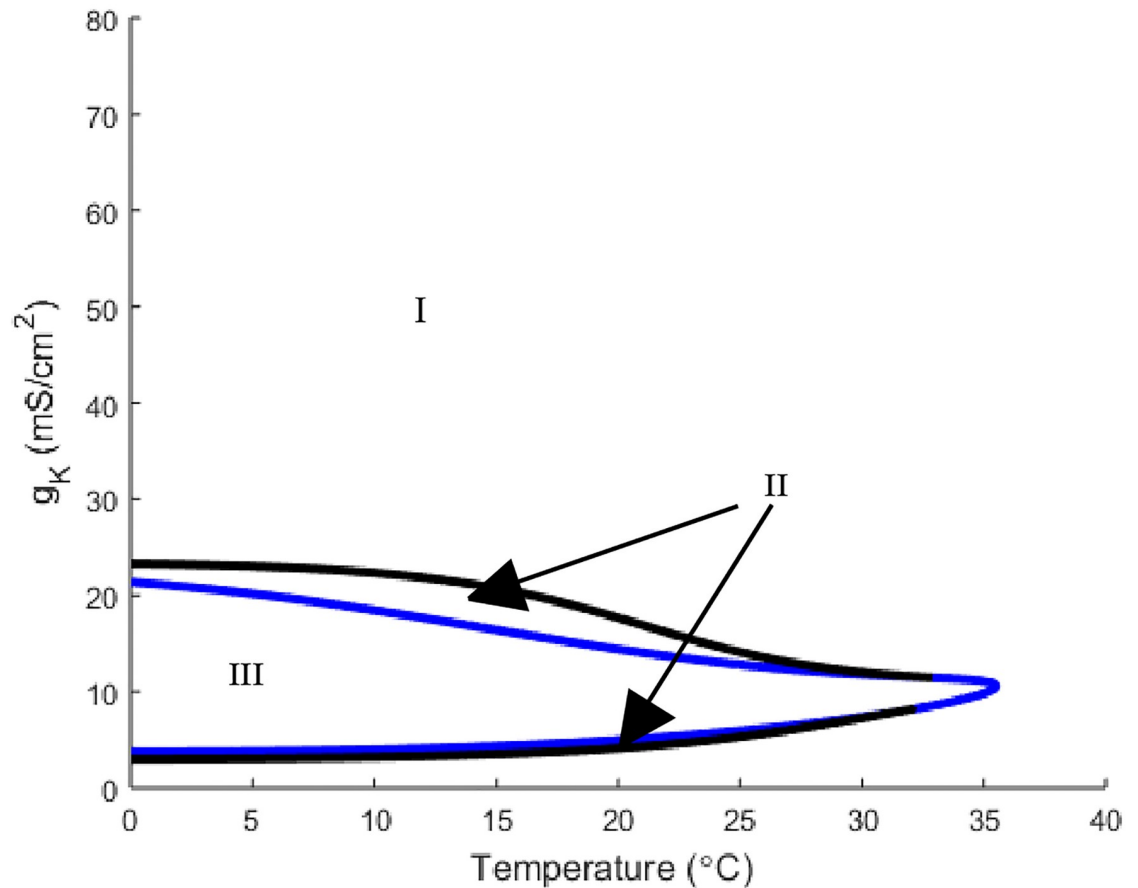


Fig 1. A two parameter bifurcation diagram of the Hodgkin-Huxley model depicting the relationship between temperature and g_K . The blue curve represents the Hopf bifurcation while the black curve is a saddle-node-periodic (SNP) bifurcation. In region I there are no oscillatory solutions and only a stable steady state solution. In region II there is a stable and an unstable oscillatory solution in addition to a stable steady state solution. Region III has a stable oscillatory solution coexisting with an unstable steady state solution.

<https://doi.org/10.1371/journal.pone.0237347.g001>

cross the blue (Hopf) curve into region III resulting in the unstable oscillatory solution disappearing. This analysis is encapsulated by the horizontal and vertical one parameter slices of this bifurcation diagram depicted in Fig 2.

The one parameter slices contain three regions of interest and four curves to keep track of. The regions are determined by the varying parameter along the x axis with all other parameters fixed for these plots. In region I we have only a stable steady state solution indicated by the red curve. In region II the steady state is still stable but there is an appearance of a stable oscillatory solution whose amplitude is indicated by the green curve and an unstable oscillatory solution which has an amplitude indicated by the dotted blue curve. The final region III transitions to an unstable steady state with a stable periodic solution whose amplitude is the green dashed curve. These slices also showcase the Hopf bifurcation point which occurs at the meeting between black and red curves and a SNP point which occurs at the meeting between blue and green curves. Fig 2 shows more explicitly the features of the neuron's membrane potential, V , in response to parameter changes. It is important to note that for the top panel in Fig 2, g_K was decreased to 20 for any activation of the neuron to occur while recalling that the standard Hodgkin-Huxley value of g_K is 36.

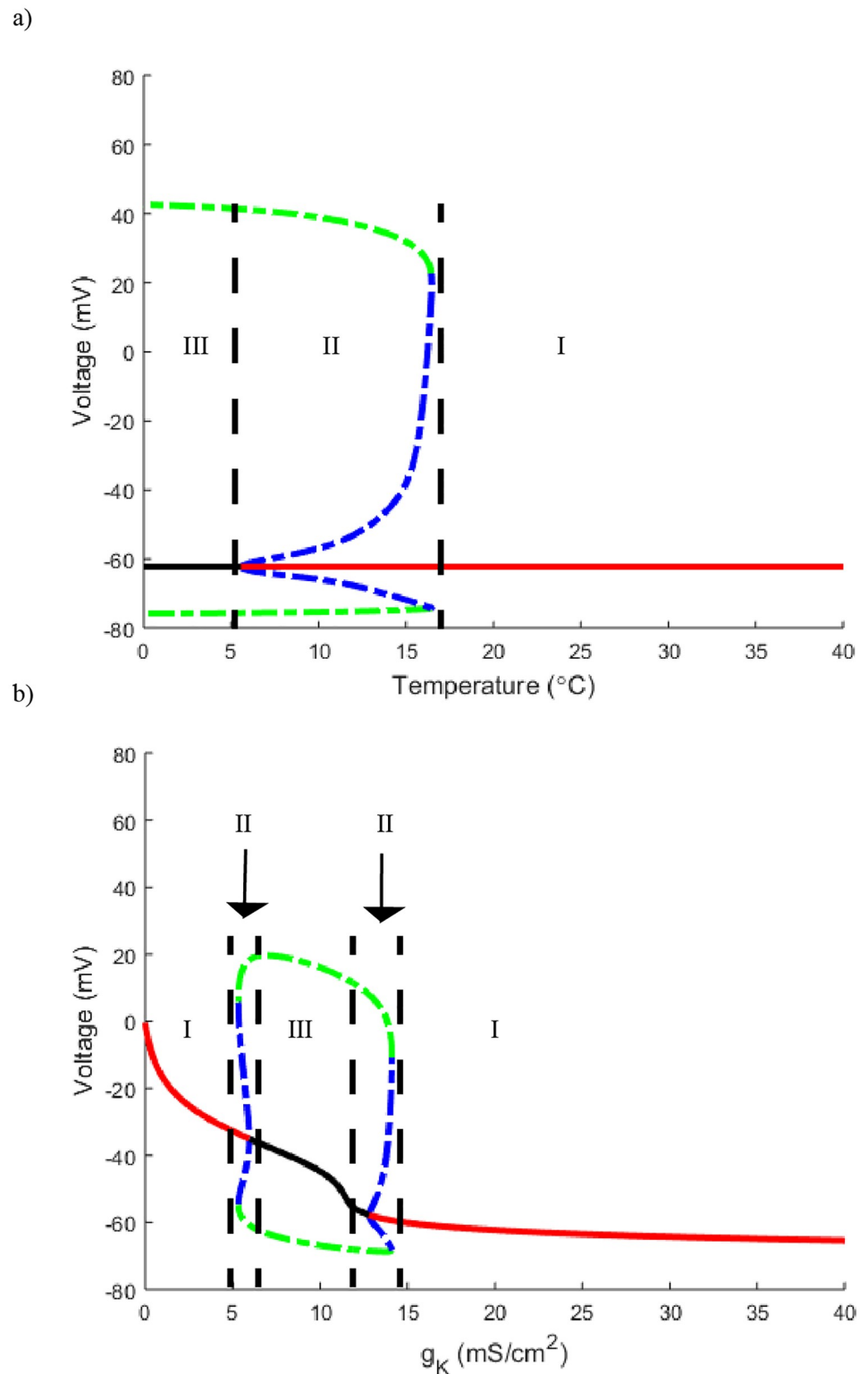


Fig 2. One parameter bifurcation slices of Fig 1. a) Horizontal slice through Fig 1 with g_K set to 20, b) a vertical slice with temperature set to 25°C. The red curve corresponds to a stable steady state while the solid black curve represents an unstable steady state. The meeting point corresponds to a Hopf bifurcation with the blue and green curves denoting the amplitudes of the unstable and stable oscillatory solutions respectively. Regions are divided by dashed black lines. Region I corresponds to a regime with a single, stable steady state solution. In region II we have a stable steady state solution with a stable (green curve) and unstable (blue curve) oscillatory solution. In region III the oscillatory solution is stable with an unstable steady state solution.

<https://doi.org/10.1371/journal.pone.0237347.g002>

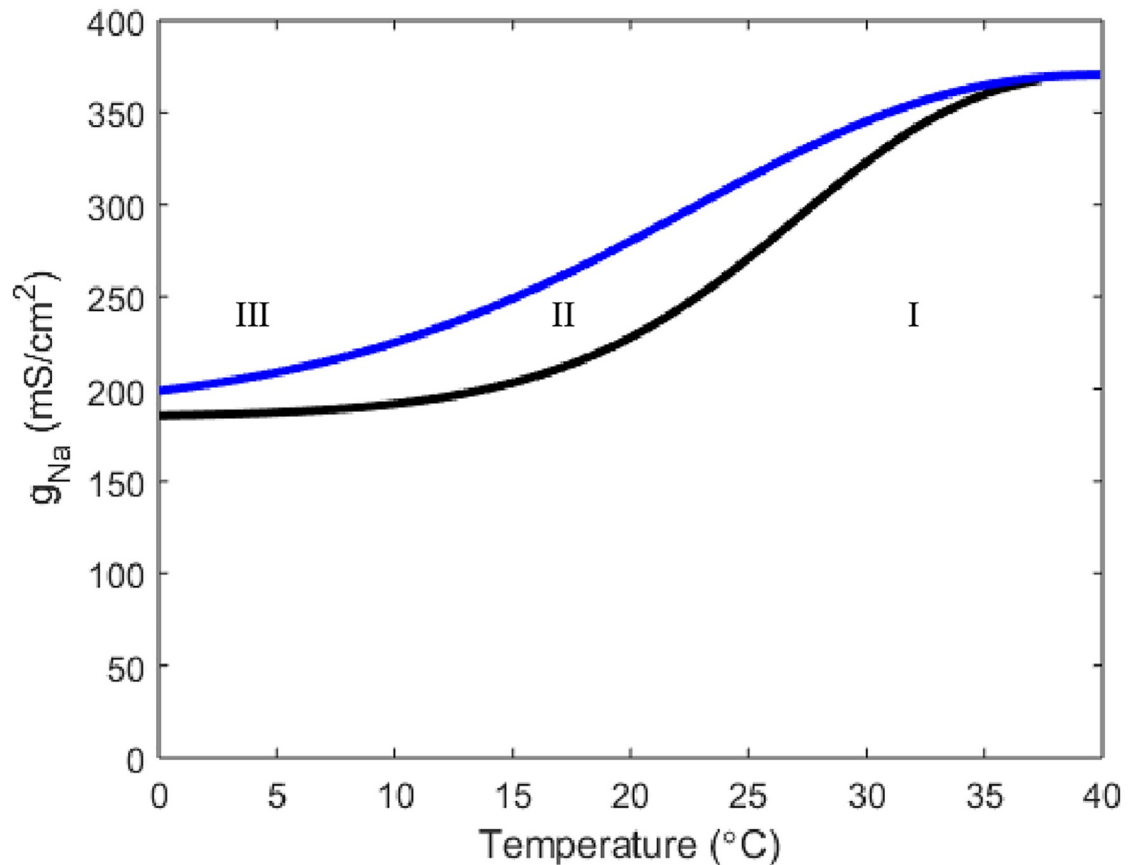


Fig 3. A two parameter bifurcation detailing the relationship between sodium maximal conductance, g_{Na} and temperature. The curve color and regions drawn are the same in meaning to those from Fig 1. Here $g_K = 36$ and $g_l = .3$.

<https://doi.org/10.1371/journal.pone.0237347.g003>

The Hodgkin-Huxley framework also allows for an exploration of the ionic currents that haven't been previously explicitly stated to have roles in threshold determination. If we adjust the leak current maximal conductance g_l but keep g_K and g_{Na} at the Hodgkin-Huxley values, no temperature dependence can be found. Alternatively, an increase of the sodium current maximal conductance can give rise to temperature responsiveness (Fig 3).

While there exist oscillatory regimes in Fig 3, they don't arise unless g_{Na} is increased well above the Hodgkin-Huxley physiological value of $g_{Na} = 120$. Furthermore, at the first value for g_{Na} where periodic solutions arise, the oscillations only result from crossing a SNP, meaning depending on initial data the solution could be oscillatory or at stable steady state resting potential. Once g_{Na} reaches close to 200 at extreme low temperatures the neuron has crossed the Hopf bifurcation and into a region where the only stable solution is oscillatory.

Next, we add in the TRPM8 component of the model by making g_{m8} nonzero. We begin by showing a plot of the open probability of TRPM8 channels, a_{m8} , in response to temperature at different physiological voltages (Fig 4). Fig 4 gives a rough idea of how the TRPM8 current will respond to temperature and voltage which combined with the voltage simulation in Fig 5 helps describe the neuron's overall behavior at different temperature levels.

From Fig 5 a few noticeable features arise as the fixed temperature level is decreased. With decreasing temperatures the simulation reveals decreasing amplitudes of the action potentials as a result of decreasing the maximum voltage attained (Fig 5). Additionally, the overall

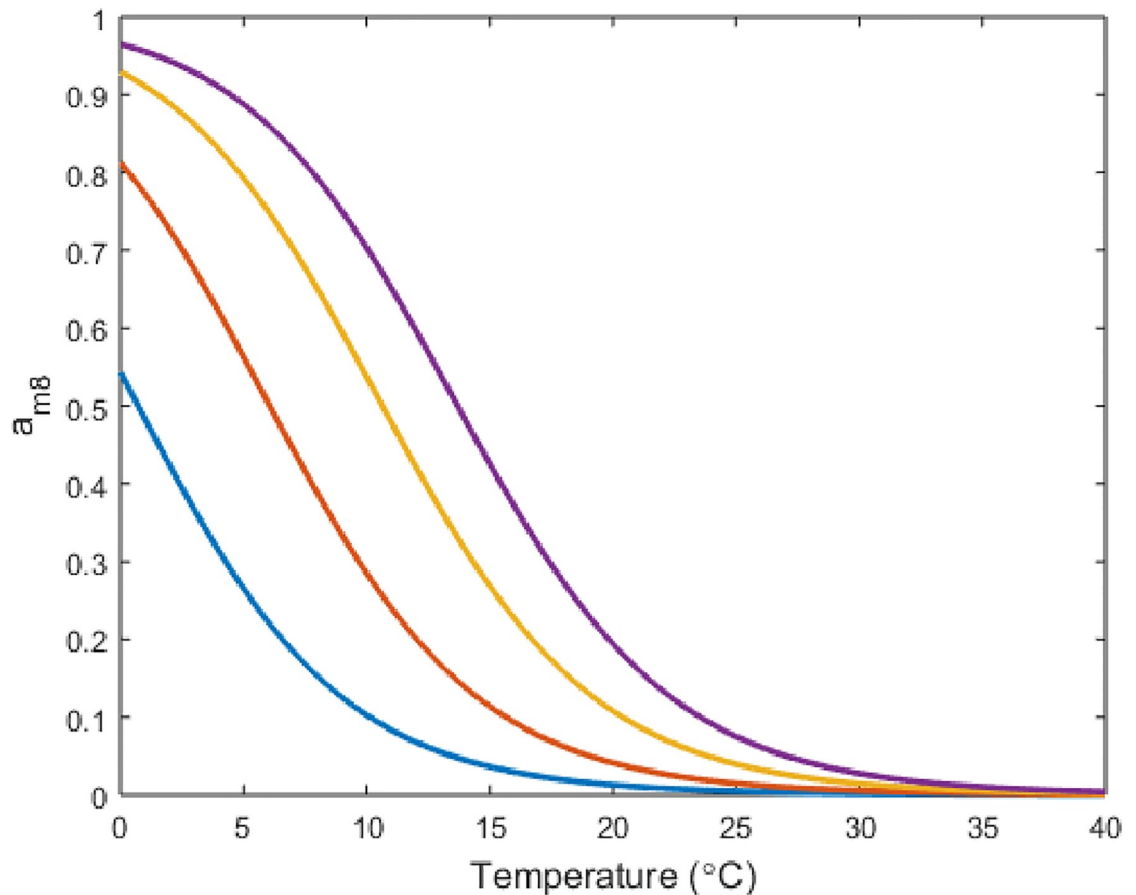


Fig 4. TRPM8 channel open probability plotted in response to temperature. Curve color corresponds to different membrane potential levels of -65mV (blue), -30mV (red), 0mV (yellow) and 20mV (purple).

<https://doi.org/10.1371/journal.pone.0237347.g004>

amplitude of the TRPM8 current continues to grow with decreasing temperatures. We note that since $E_{m8} = 0$ this allows for the TRPM8 current to be both inward and outward depending on the membrane potential. The change in TRPM8 current amplitude is mainly due to the increase in inward flux, although it is noteworthy that at 8°C and 12°C there's an increase in outward current. It is also informative to examine the behavior as g_{m8} is increased in response to a simulated temperature ramp (Fig 6).

Across the three different values of g_{m8} there are two consistent features, and one that arises as g_{m8} is increased. In all three plots there are large amplitude jumps in the oscillations when the neuron first turns on and when it turns off. Furthermore, in each of the three plots, the neuron's activity on the down ramp and up ramp of temperature appear asymmetric, with the oscillations on the increasing temperature ramp lasting longer. Finally, as g_{m8} is increased, the neuron ceases to have oscillations in the coldest temperature portion of the ramp. The plots with $g_{m8} = 5$ and $g_{m8} = 10$ also show how the oscillations shrink in amplitude as the neuron is exposed to decreasing temperatures.

Although these Voltage-Time plots give a general idea of the effect that TRPM8 channels have on the neuron's activation and inactivation, we wish to give fuller explanation of the interplay between each of the ionic currents and temperature. In Fig 7 we focus on g_{m8} and its relationship with temperature in a two parameter bifurcation diagram. Critically, with $g_K = 36$, the standard Hodgkin-Huxley value, starting in region I on the right (30°C) and decreasing

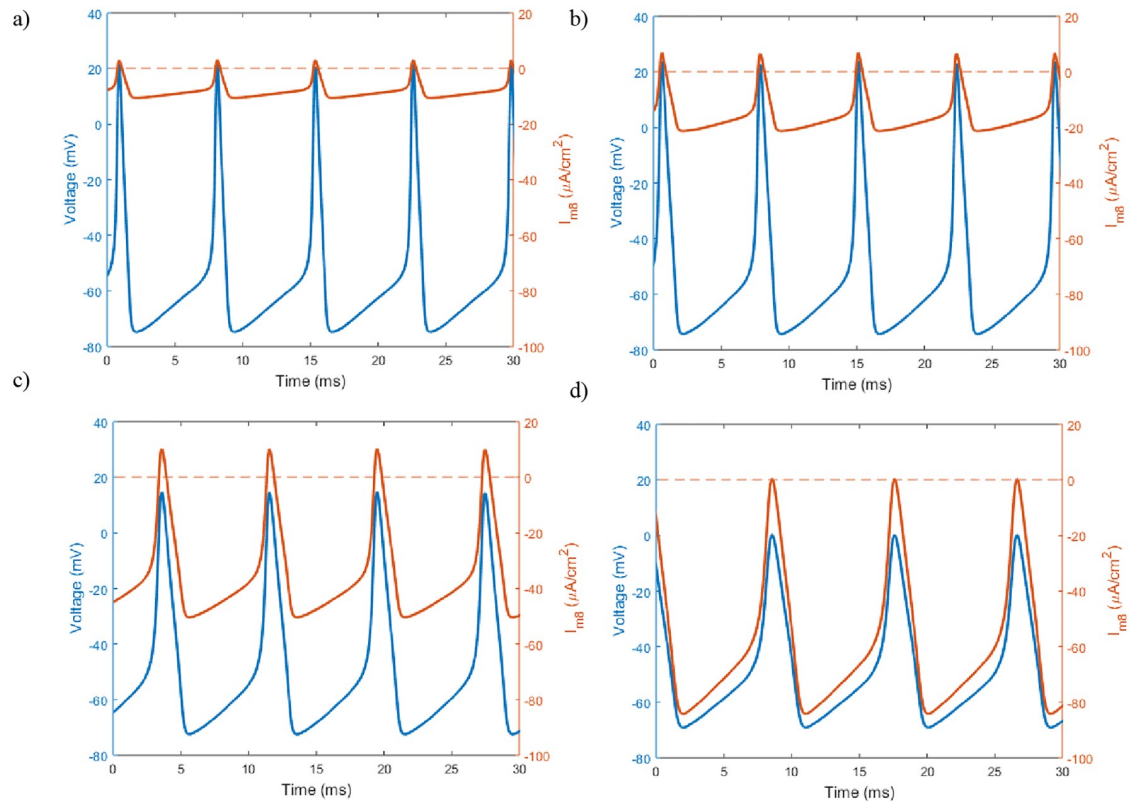


Fig 5. Sample traces of the neuron's membrane potential and TRPM8 current in response to different static temperature levels. a-d) Temperature is set to 15°, 12°, 8° and 5° Celsius respectively. The membrane voltage is in blue with the TRPM8 current overlaid in red. The red dashed line denotes where the TRPM8 current switches from inward (negative values) to outward (positive values). Here $g_{m8} = 3$ and all other parameter values are set to Hodgkin-Huxley standards.

<https://doi.org/10.1371/journal.pone.0237347.g005>

temperature turns on the neuron by crossing through the SNP bifurcation and then the Hopf bifurcation. We highlight the importance of the SNP bifurcation and region II in general as the existence of the unstable oscillatory solution implies that a slight perturbation or input could turn the neuron on from the stable steady state. Looking at horizontal slices of this two parameter bifurcation in Fig 7 we easily see the shift of the temperature threshold. Changing $g_{m8} = 3$ to $g_{m8} = 50$ from Fig 8a to 8b changes how much less temperature must drop to turn the neuron on with higher g_{m8} values.

Returning to the high versus low threshold phenomenon, keeping otherwise standard Hodgkin-Huxley parameter values, increasing g_{m8} shifts the neuron from a higher to a lower activation threshold (Figs 7 and 8). Additionally, with $g_{m8} = 3$ we can consider traveling horizontally through Fig 9 at values $g_K = 45$ and $g_K = 20$. This shows that decreasing g_K shifts the Hopf and SNP curves further right thus requiring a lower drop in temperature in order to turn on. A representative vertical slice in Fig 10 showcases the transitions from stable steady state solution to oscillatory and back.

To summarize the relationship between TRPM8 and voltage gated potassium channels, plots of g_{m8} against g_K at four different temperature values are provided in Figs 11 and 12. The first observation is that the total area of parameter space in which there are oscillations decreases as temperature decreases. Yet in spite of this, each plot has the feature that starting in region III, where there are oscillatory solutions, and decreasing g_{m8} takes the neuron to region I where there are no periodic solutions. This can then be counterbalanced by decreasing g_K to

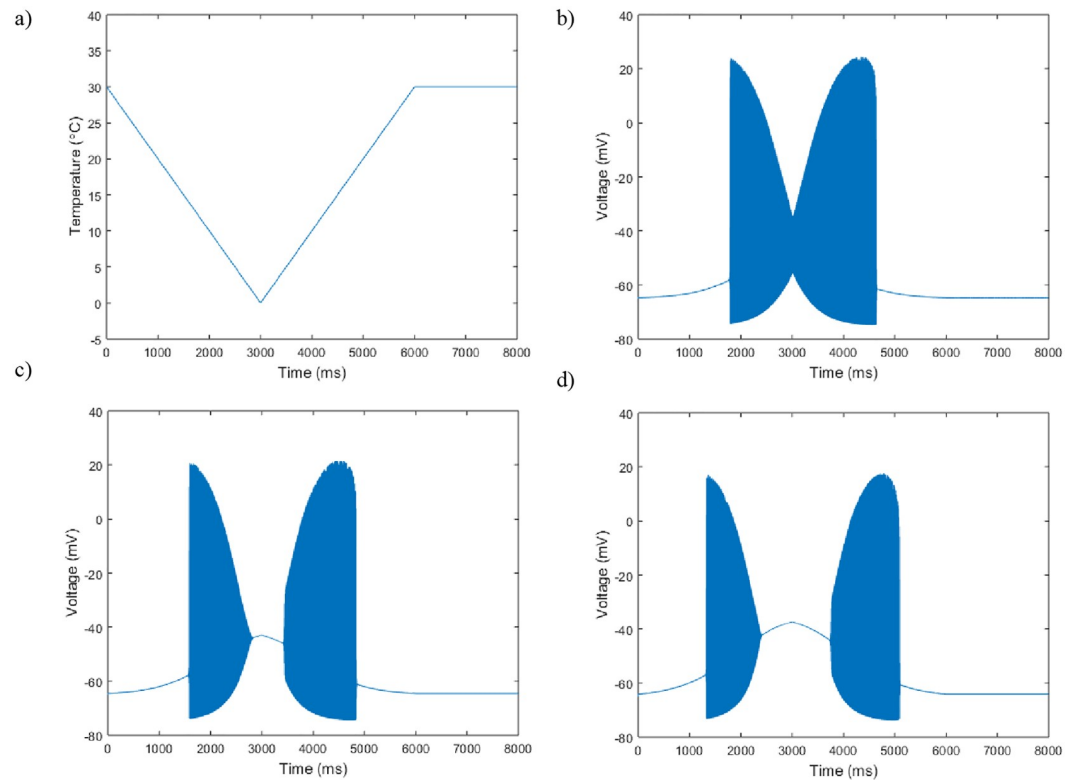


Fig 6. Membrane potential plotted against time in response to a simulated temperature ramp. a) The simulated change in temperature over time. b) The neuron's periodic spiking behavior response to the temperature change plotted against time with $g_{m8} = 3$. c) Here $g_{m8} = 5$. d) Here $g_{m8} = 10$. All other parameter values are set to Hodgkin-Huxley values.

<https://doi.org/10.1371/journal.pone.0237347.g006>

take the neuron back into region III. Similar transitions between regions takes place if g_K is decreased first followed by a decrease in g_{m8} (Figs 11 and 12).

With a clearer idea of how the TRPM8 current interacts with temperature and the potassium current to determine the threshold level we turn to the sodium and leak currents. By increasing g_{m8} we can see the relationship temperature has with g_{Na} (Fig 13).

At these low values of g_{m8} we see similar behavior to Fig 3. Of note, the neuron now does turn on in the horizontal slice of $g_{Na} = 120$, but this still occurs only at extreme low temperatures. Furthermore we still see that for a tiny window of g_{Na} values we can obtain periodic solutions that are only a result of the SNP. Yet if we increment g_{m8} further we can see temperature specific windows of periodic solutions arise (Fig 14).

We see that with $g_{m8} = 3$, at values for g_{Na} between 60 and 100, horizontal slices result in the neuron turning on and off again at specific temperatures. Further emphasis of how these neurons' temperature responses can be finely tuned is shown for $g_{m8} = 10$. Horizontal slices at different g_{Na} values through Fig 14b reveal temperature windows of different lengths and of different intervals. A similar observation can be made about the effect the leak current has on the neuron's degree of response (Fig 15).

Taking a horizontal slice with $g_l = .3$ as it is in the canonical Hodgkin-Huxley formulation we have temperature sensitivity. Yet as with the sodium current, we can tune the width of temperature range in which this neuron is active by increasing g_l .

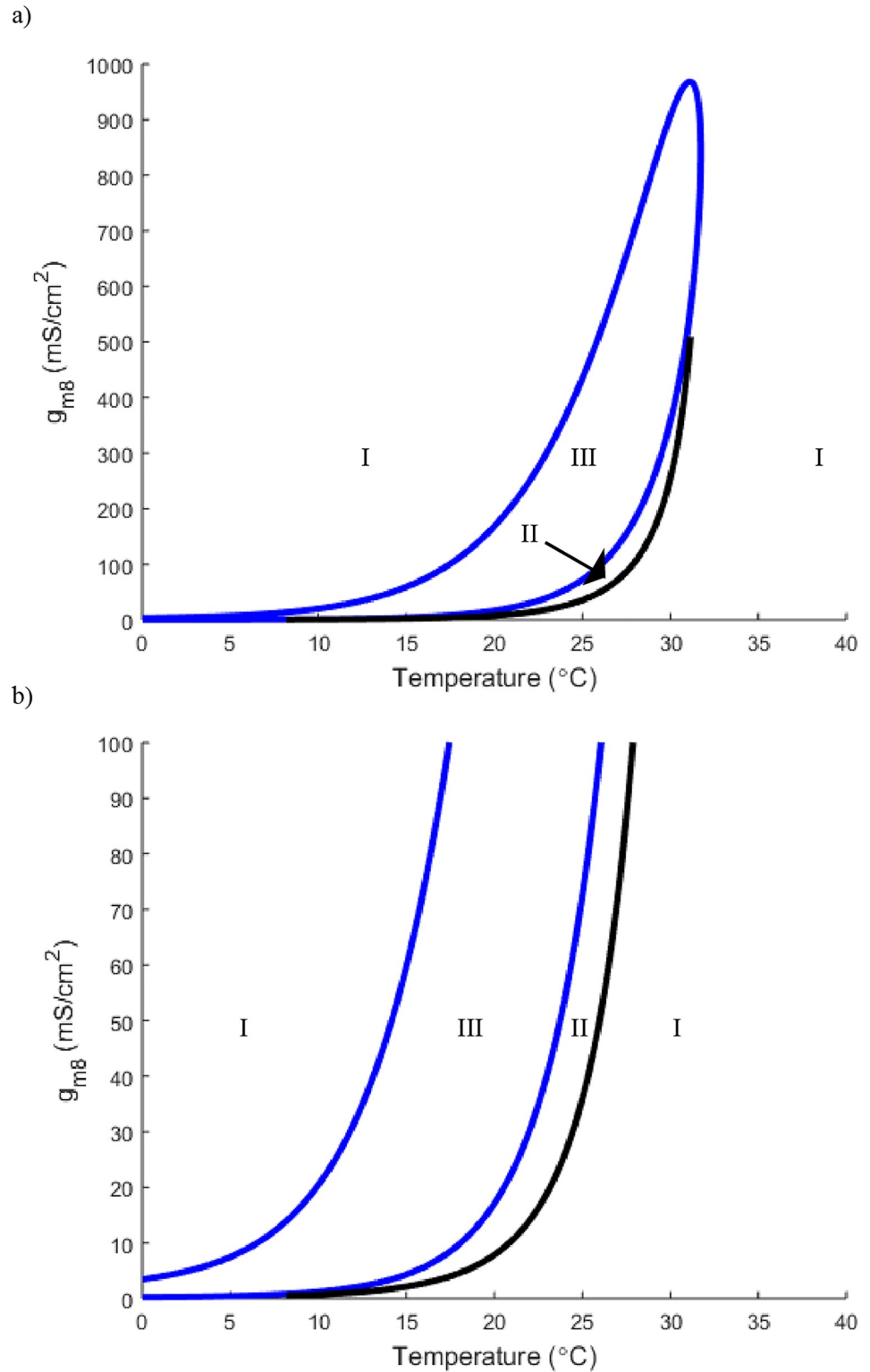


Fig 7. a) A two parameter bifurcation demonstrating the relationship between temperature and g_{m8} . b) a zoomed in version of Fig 6a. As in Fig 1, The blue curve represents the Hopf bifurcation while the black curve is a saddle-node-periodic (SNP) bifurcation. The regions are labeled as in Fig 1. Here g_K is set to 36.

<https://doi.org/10.1371/journal.pone.0237347.g007>

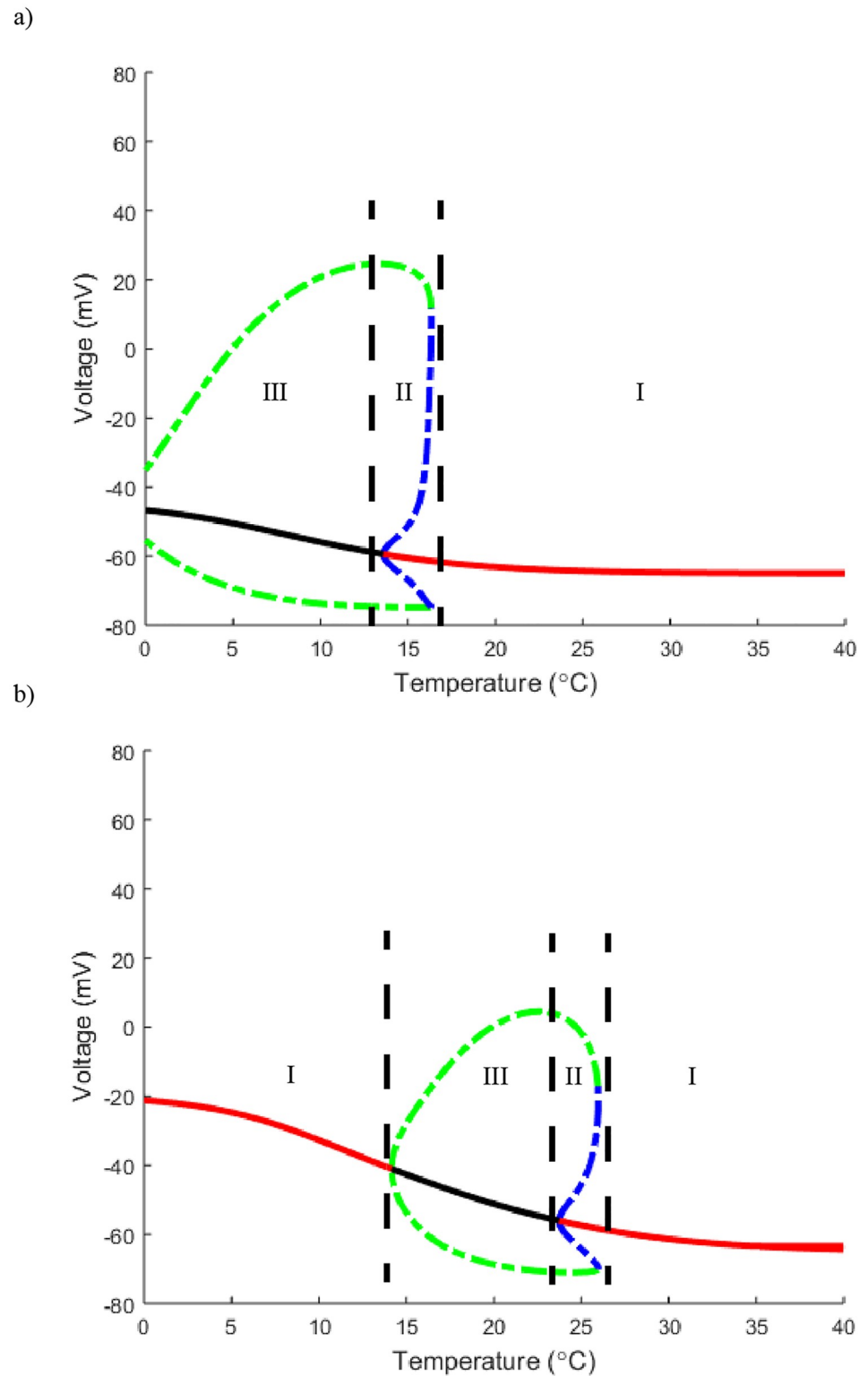


Fig 8. Horizontal one parameter bifurcation slices of Fig 6. a) A slice with g_{m8} set to 3. b) A horizontal slice with g_{m8} set to 50. In both a) and b) $g_K = 36$. Curve color and labeled regions are identical in meaning to those in Fig 2.

<https://doi.org/10.1371/journal.pone.0237347.g008>

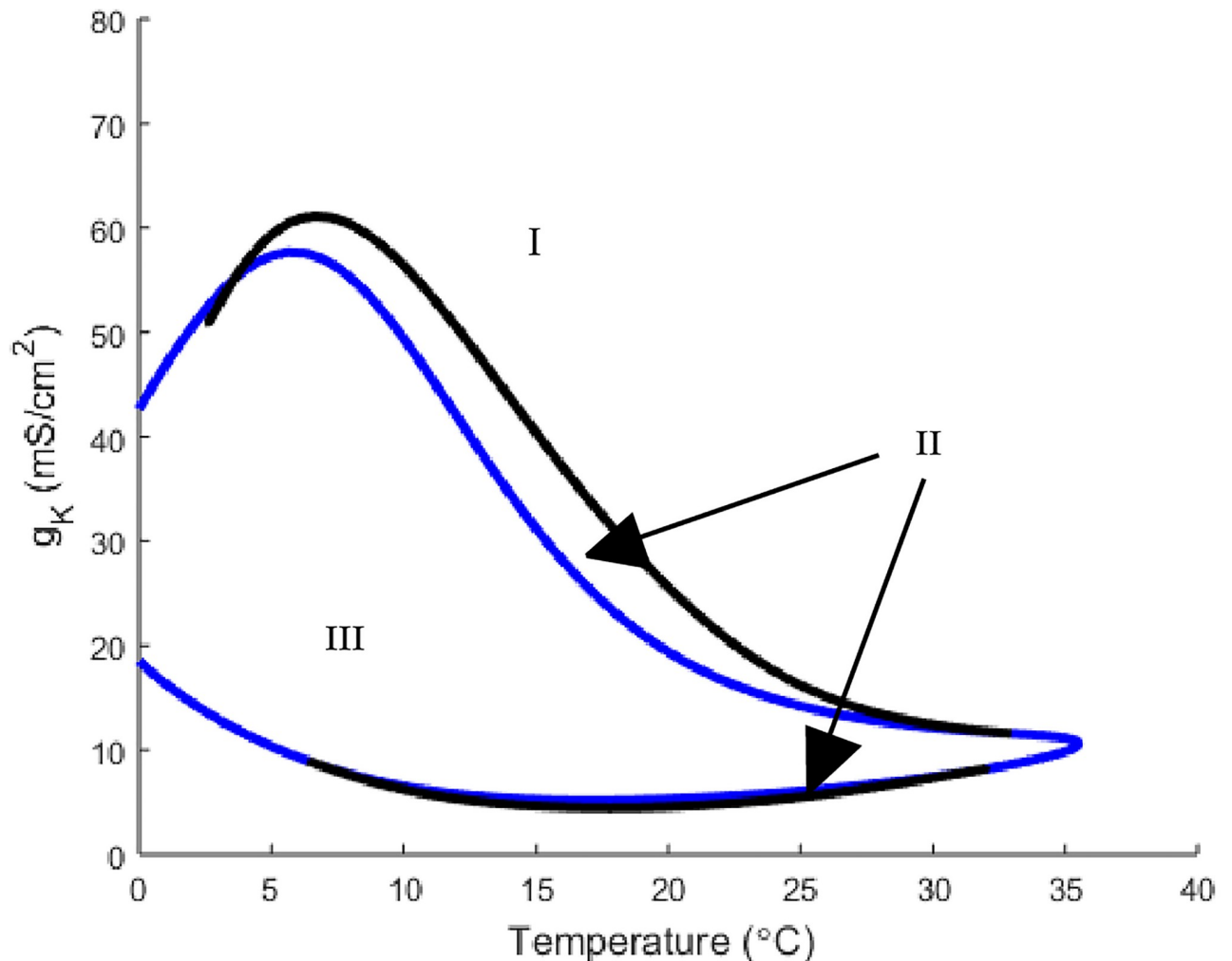


Fig 9. A two parameter bifurcation of the relationship between temperature and g_K . Curve color and labeled regions are identical in meaning to those in Fig 1. Here $g_{m8} = 3$.

<https://doi.org/10.1371/journal.pone.0237347.g009>

Discussion

As advancements are made in the field of neuroscience, labs are beginning to examine properties of a variety of different neuron classes. One of the classes that garnered some interest recently was cold thermosensors. Particular attention was given to the role of their ion channels, critically the TRPM8 and voltage gated potassium channels. Here we have developed a simple model of a cold thermosensor centered around a Hodgkin-Huxley base with an added TRPM8 component. The goal here was to create a physiological model that would allow for investigation into the roles and properties of the involved ion channels and how they interact with changes in temperature.

The first point we emphasize is that the Hodgkin-Huxley model at standard parameter values does not have sufficient temperature dependence to account for the known data. Adding a TRPM8 channel to the model results in the appearance of oscillatory solutions for the neuron with temperature decrease (Figs 8 and 9). This coincides with lab findings highlighting the importance of TRPM8 channels within the class of cold thermosensors [2, 4, 5]. Previous work

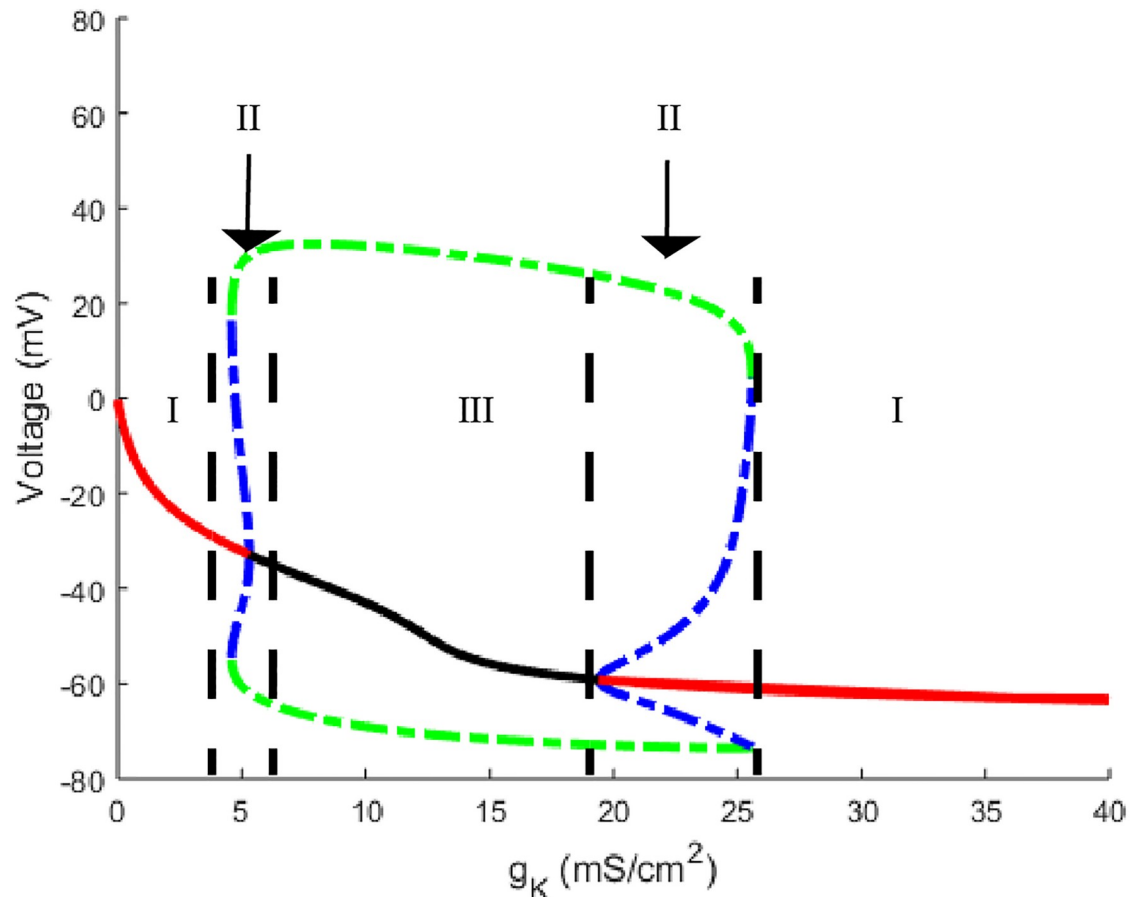


Fig 10. A horizontal slice from Fig 8. Temperature is set to 20 degrees Celsius and g_{m8} is set to 3. Curve color and labeled regions are identical in meaning to those in Fig 2.

<https://doi.org/10.1371/journal.pone.0237347.g010>

also highlights the variety of cold sensing neurons describing a range from high to low threshold neurons with a range of activation temperatures [3, 5]. One defining characteristic that separated high from low threshold was found to be the effectiveness of the TRPM8 channels [2, 8]. With a higher density of TRPM8 channels, the neuron can activate at higher temperature values [8]. Our model has this same graded temperature threshold showing that a change in maximal conductance of TRPM8 channels changes how far temperature must drop to obtain an oscillatory solution. Specifically, we show that at otherwise standard Hodgkin-Huxley parameter values with $g_{m8} = 3$ the temperature threshold is 15°C to turn on while at $g_{m8} = 50$ the threshold is 25°C (Figs 7 and 8).

We also demonstrate what the oscillation profiles look like in response to different temperature levels. We show how the changes in the neuron's behavior is dependent on the growth of the TRPM8 inward current (Fig 5). The temperature ramp simulation with increasing TRPM8 maximal conductance helps give a clearer view of the response of what the neurons are physiologically exposed to (Fig 6). Figs 5 and 6 help provide insight into the cold receptor's activation and inactivation in response to increasing and decreasing temperatures.

Although TRPM8 channels were identified as a main determining factor in the identification of cold thermosensors, many labs also highlight the importance of voltage gated potassium channels [2, 8]. While previous mathematical models of cold sensors had the desired

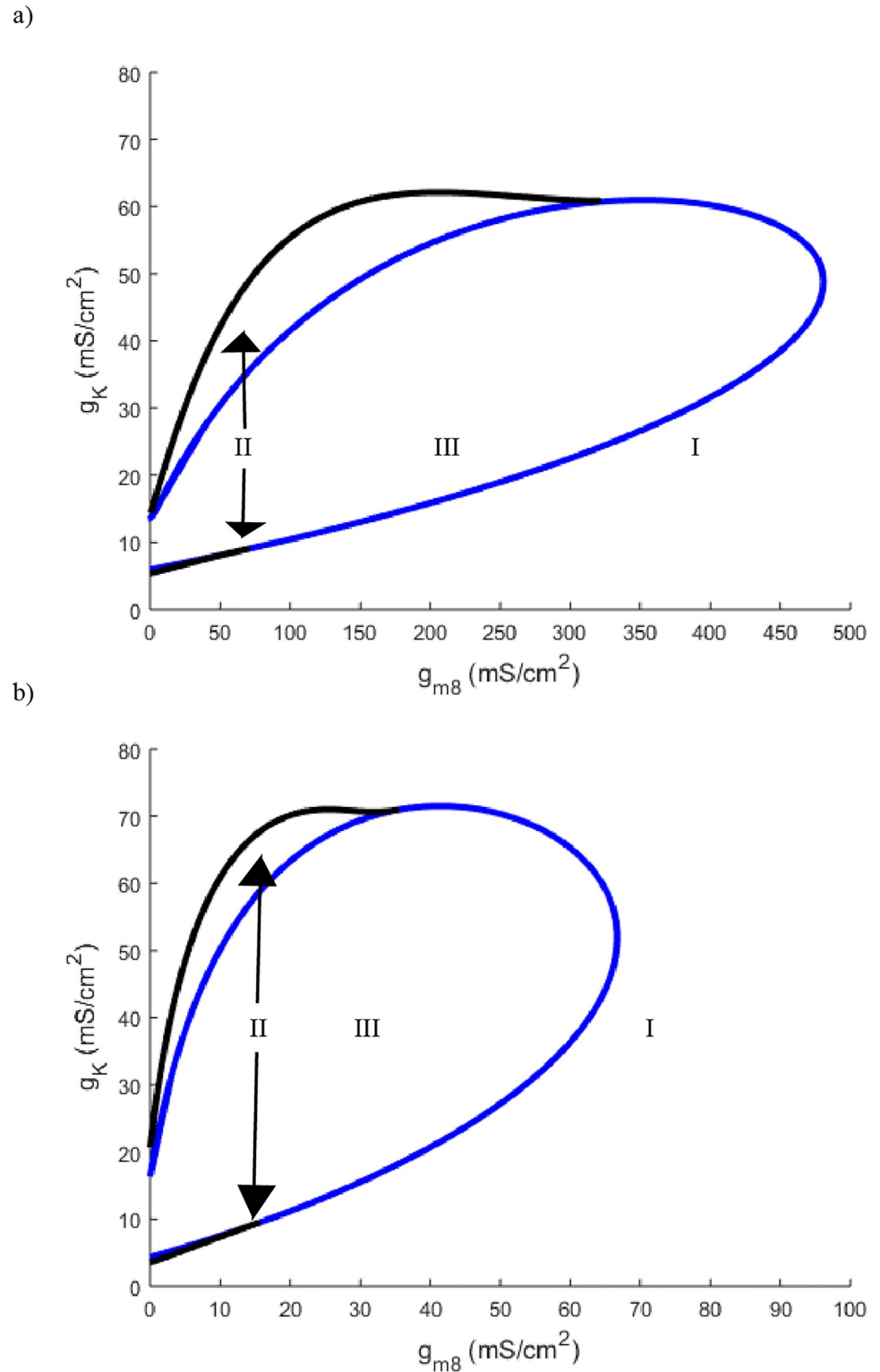


Fig 11. a) Two parameter bifurcation of g_{m8} plotted against g_K with temperature set to 25°C. b) Two parameter bifurcation of g_{m8} plotted against g_K with temperature set to 15°C. Curve color and labeled regions are identical in meaning to those in Fig 1.

<https://doi.org/10.1371/journal.pone.0237347.g011>

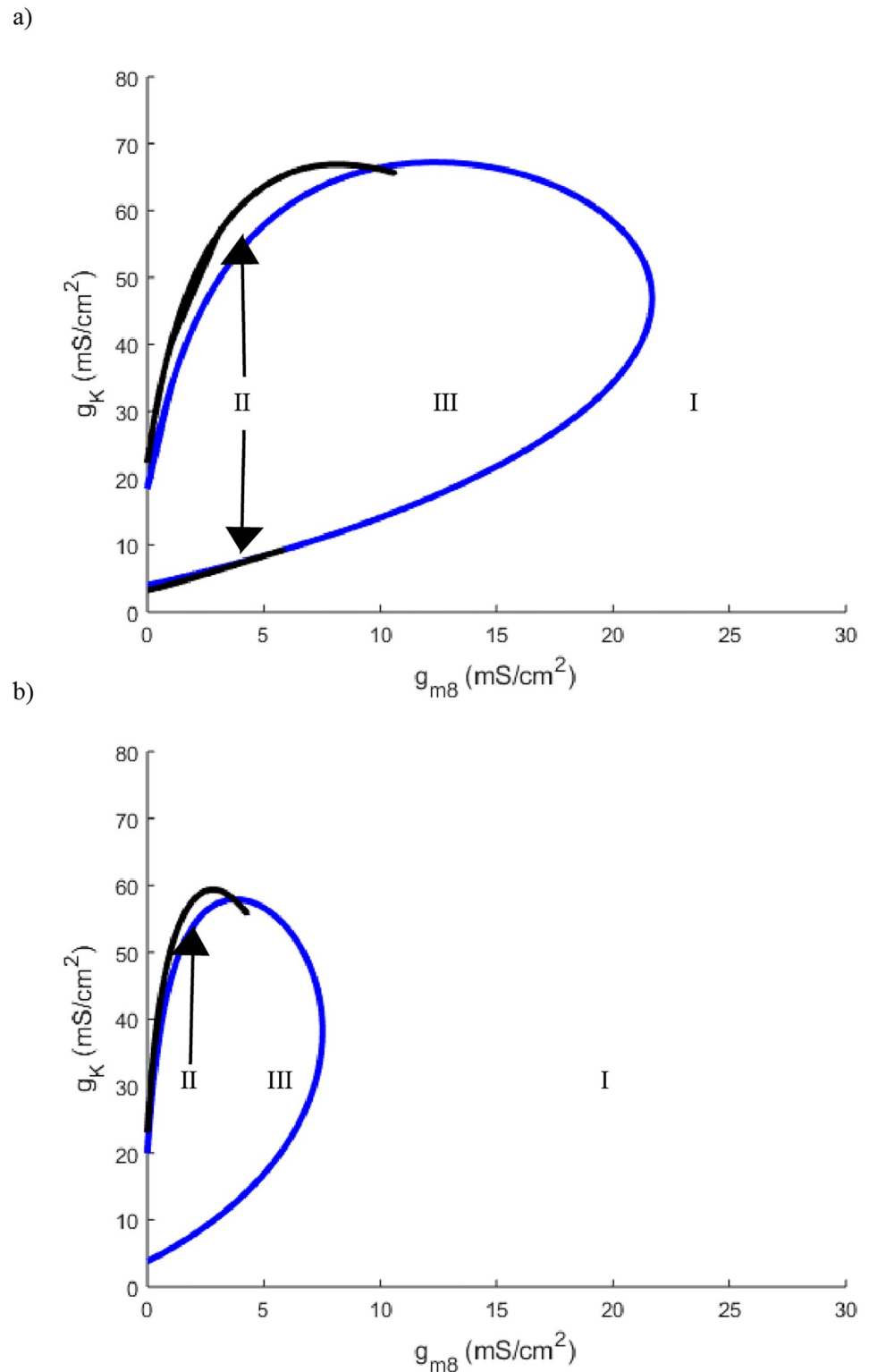


Fig 12. a) Two parameter bifurcation of g_{m8} plotted against g_K with temperature set to 10°C . b) Two parameter bifurcation of g_{m8} plotted against g_K with temperature set to 5°C . Curve color and labeled regions are identical in meaning to those in Fig 1.

<https://doi.org/10.1371/journal.pone.0237347.g012>

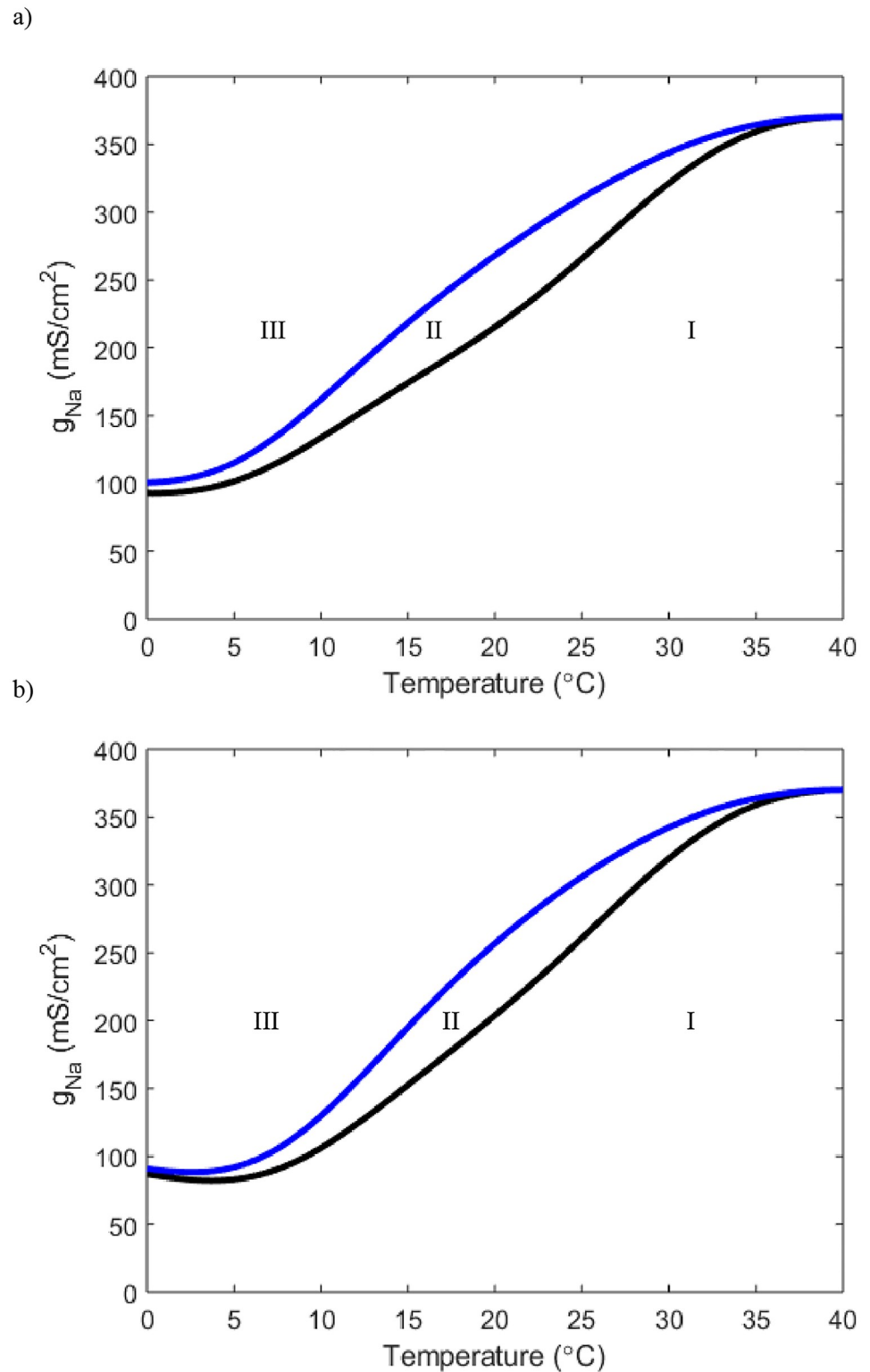


Fig 13. Two parameter bifurcations showing the relationship between temperature and g_{Na} . In the top plot $g_{m8} = .5$ and in the bottom $g_{m8} = 1$. Both g_j and g_K are set to Hodgkin-Huxley values. Curve color and region meaning is equivalent to other two parameter bifurcation plots.

<https://doi.org/10.1371/journal.pone.0237347.g013>

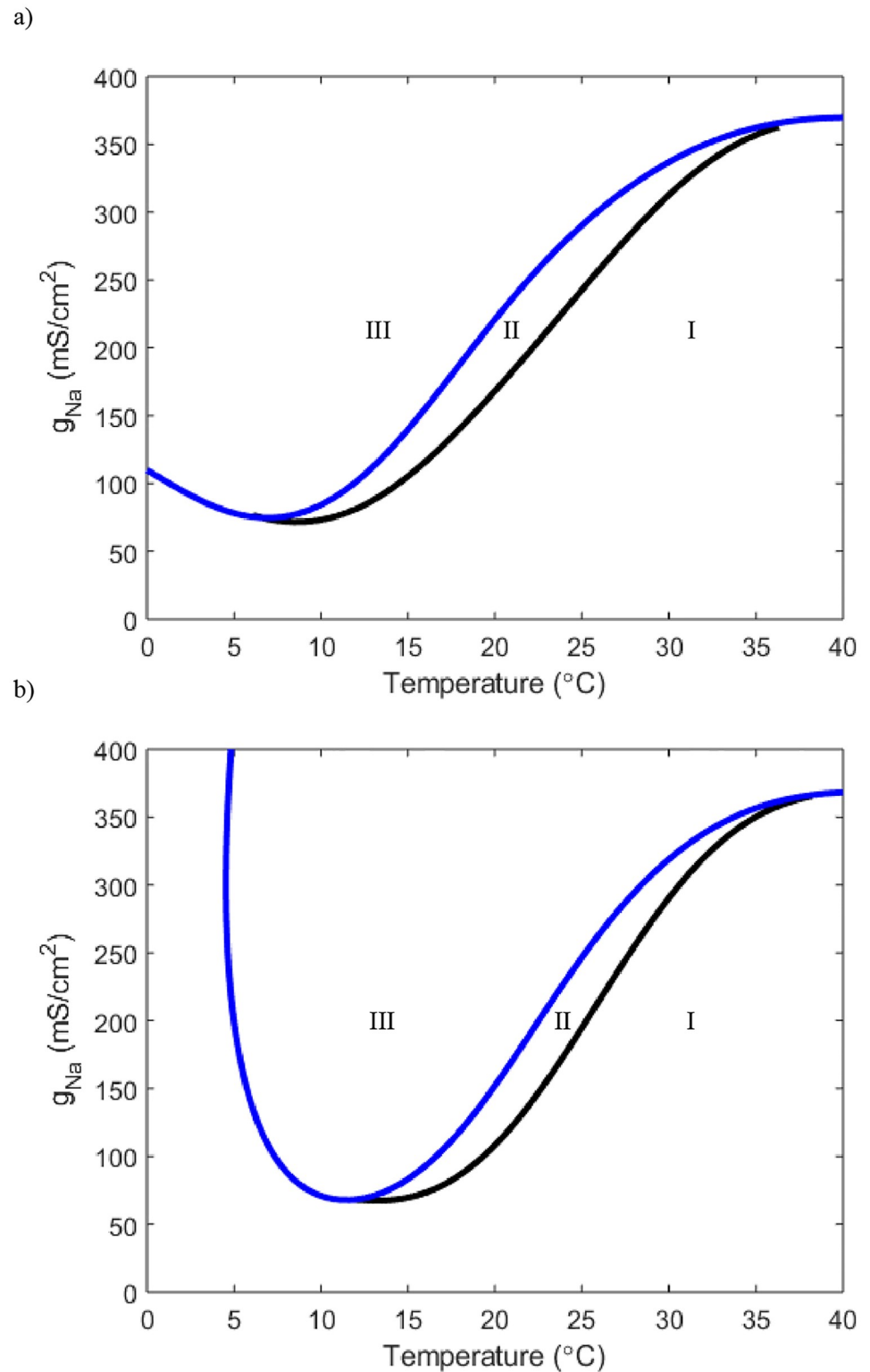


Fig 14. Two parameter bifurcations showing the relationship between temperature and g_{Na} . In the top plot $g_{ms} = 3$ and in the bottom $g_{ms} = 10$. Both g_l and g_K are set to Hodgkin-Huxley values. Curve color and region meaning is equivalent to those in Fig 1.

<https://doi.org/10.1371/journal.pone.0237347.g014>

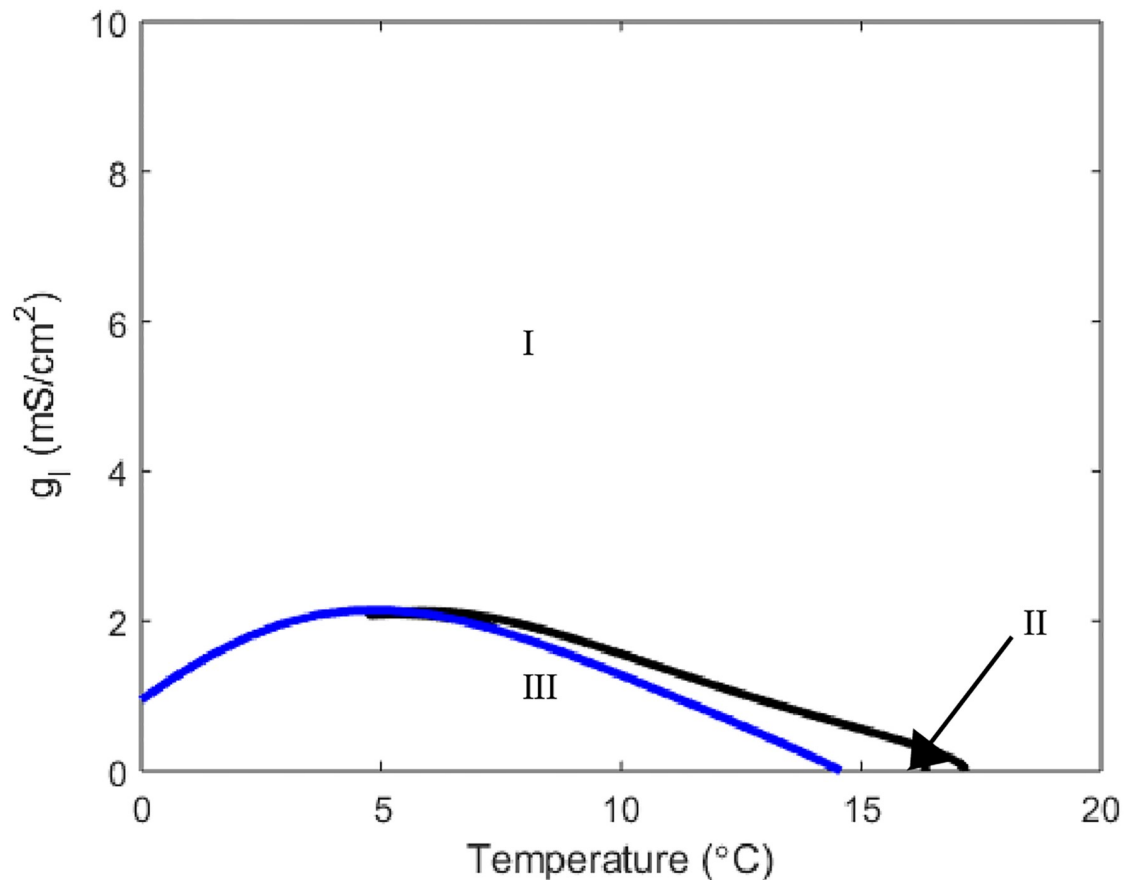


Fig 15. Two parameter bifurcation plot relating g_l to temperature. Here $g_{m8} = 3$. All other parameters are set to Hodgkin-Huxley value with curve color and region meaning equivalent to those in Fig 1.

<https://doi.org/10.1371/journal.pone.0237347.g015>

response to the lowering of temperature, they lacked the ability to track specific ionic currents [10]. With the Hodgkin-Huxley model as a basis for our model, the potassium flux was able to be explicitly tracked. Altering the potassium channel maximal conductance also found the model to be in agreement with previous lab findings. Lowering the maximal conductance of potassium channels g_K , can transition the neuron from high to low threshold (Fig 9). Also shown in lab settings, TRPM8 and voltage gated potassium channels have offsetting effects [8]. If TRPM8 maximal conductance is lowered, the neuron can be made non-responsive to temperature as seen in Figs 11 and 12 by going from region III to I. This can then be reversed by decreasing the potassium maximal conductance which takes the neuron back into region III. We note that this counterbalancing effect stems primarily from g_K being an outward current with g_{m8} being a largely inward current due to their reversal potentials. Thus this offsetting affect may be a general feature due more to the ion channel current directions than to specific ion channel type.

Our modelling framework simultaneously allows for exploration of the effects of the sodium and leak currents. The sodium current does not appear to have a role in setting the threshold level. For the sodium current, with $g_{m8} = 0$, the neuron will only activate in the extreme temperature range and not until g_{Na} is drastically increased away from Hodgkin-Huxley value (Fig 3). We also notice that not until $g_{m8} = 3$ does the neuron have stable oscillatory solutions from crossing a Hopf bifurcation point near values of $g_{Na} = 120$ (Figs 13 and 14).

Although the sodium current does not appear to heavily dictate the threshold level for activation, it appears to have some control over the range of temperature the neuron can sense (Figs 13 and 14). After g_{m8} is increased above 3, we see that different horizontal slices yield different temperature windows of activation and inactivation (Fig 14b). This implies that the specificity of exactly when the cold thermosensors turn on and off may be modulated by the number of sodium channels present.

This temperature window feature is also observable with alterations to the leak current maximal conductance. In particular with $g_l = .3$ as it is in Hodgkin-Huxley and $g_{m8} = 3$ we see the neuron turns on and stays on past 0°C (Fig 15). Yet increasing g_l to be between 1 and 2 we can see that for a horizontal slice we have a temperature value in which oscillatory solutions arise and then a second temperature before 0°C where the neuron returns to a stable steady state solution (Fig 15). The analysis of the sodium and leak currents indicates while the main threshold level is set by the relationship between the TRPM8 and potassium currents, these currents may still have a role to play. Finely tuned temperature responses may be dictated by the strength of the sodium and leak currents.

Finally, while the majority of previous work centered upon investigating at what point these cold sensing neurons turn on, this model provides additional insight into the neuron's inactivation. Fig 4 shows the TRPM8 current is activated at these lower temperature for all relevant voltages. However, in Figs 5 and 6, we can see the full behavior of the neuron at these lower temperatures, with a decrease in spiking amplitude height corresponding to an increase in inward TRPM8 current. From Fig 7 we see that if g_{m8} is fixed at any value near or above 10, lowering temperature far enough will inactivate the neuron by returning it to region I. In particular, as seen in Fig 8b, region I on the left corresponds to only a single stable steady state. However, it is important to note that this steady state is at a much higher resting membrane voltage, -20mV , than the typical resting potential range of -65mV . This observation lends itself to the idea that either at extremely low temperatures the neuron is overstimulated and can no longer fire action potentials, or the current model does not include enough ion channels to fully encapsulate the behavior of cold sensing neurons in extreme temperatures.

We see a similar phenomenon at extreme low temperatures with regards to lowering g_K . In the temperature window of 0°C – 10°C , decreasing g_K causes the neuron to transition to region I with only a single steady state (Fig 9). As was seen in Fig 8 when altering g_{m8} , by decreasing g_K far enough the neuron is depolarized with a single steady state but at a much higher value, near -20mV , than a standard Hodgkin-Huxley neuron resting potential (Fig 10). These observations are corroborated by Figs 11 and 12 which highlight that as temperature decreases towards the extreme, the total area of region III decreases drastically. From this we can hypothesize that either the cold sensitive neurons at extremely low temperatures are extremely specific as to the densities of their ion channels, or as predicted by some, there are other channels at play including the TTX resistant $Na_v1.8$ and possibly TRPVA1 channels [5, 8, 16].

Conclusion

The general Hodgkin-Huxley structure of this model meant that specific ionic currents, could be tracked. Unlike in previous cold sensing neuron models where the types of ionic currents were not explicit, this new model allows for examination of high versus low threshold neurons and the specific temperature levels of activation and inactivation. We demonstrated the value an in-depth bifurcation analysis can provide for answering biological questions. This analysis helped solidify some of the primary features of cold sensing neurons: the presence of TRPM8 channels, different threshold neurons and the interplay between the TRPM8 current and the voltage gated potassium current. Additionally, the analysis showed that the leak and sodium

currents could act as mediators of the temperature window in which these neurons activate. By starting with a physiological basis and then adding the highlighted current TRPM8, we were able to provide an improved overall understanding of the neuron class of cold thermosensors.

Author Contributions

Conceptualization: Kees McGahan, James Keener.

Formal analysis: Kees McGahan, James Keener.

Methodology: Kees McGahan, James Keener.

Supervision: James Keener.

Writing – original draft: Kees McGahan.

Writing – review & editing: Kees McGahan, James Keener.

References

1. Teichert RW, Smith NJ, Raghuraman S, Yoshikami D, Light AR, Olivera BM. Functional profiling of neurons through cellular neuropharmacology. *Proceedings of the National Academy of Sciences*. 2012; 109(5):1388–95. <https://doi.org/10.1073/pnas.1118833109>
2. Teichert RW, Memon T, Aman JW, Olivera BM. Using constellation pharmacology to define comprehensively a somatosensory neuronal subclass. *Proceedings of the National Academy of Sciences*. 2014 Feb 11; 111(6):2319–24. <https://doi.org/10.1073/pnas.1324019111>
3. McKemy DD. The molecular and cellular basis of cold sensation. *ACS chemical neuroscience*. 2013 Feb 20; 4(2):238–47. <https://doi.org/10.1021/cn300193h> PMID: 23421674
4. McKemy DD. How cold is it? TRPM8 and TRPA1 in the molecular logic of cold sensation. *Molecular pain*. 2005 Apr 22; 1:1744–8069. <https://doi.org/10.1186/1744-8069-1-16>
5. Luiz AP, MacDonald DI, Santana-Varela S, Millet Q, Sikandar S, Wood JN, et al. Cold sensing by NaV1.8-positive and NaV1.8-negative sensory neurons. *Proceedings of the National Academy of Sciences*. 2019 Feb 26; 116(9):3811–6. <https://doi.org/10.1073/pnas.1814545116>
6. Vriens J, Nilius B, Voets T. Peripheral thermosensation in mammals. *Nature Reviews Neuroscience*. 2014 Sep; 15(9):573–89. <https://doi.org/10.1038/nrn3784> PMID: 25053448
7. Voets T, Owsianik G, Janssens A, Talavera K, Nilius B. TRPM8 voltage sensor mutants reveal a mechanism for integrating thermal and chemical stimuli. *Nature Chemical Biology*. 2007 Mar 11; 3(3):174–82. <https://doi.org/10.1038/nchembio862> PMID: 17293875
8. Madrid R, Pena EDL, Donovan-Rodriguez T, Belmonte C, Viana F. Variable Threshold of Trigeminal Cold-Thermosensitive Neurons Is Determined by a Balance between TRPM8 and Kv1 Potassium Channels. *Journal of Neuroscience*. 2009 Mar 11; 29(10):3120–31. <https://doi.org/10.1523/JNEUROSCI.4778-08.2009> PMID: 19279249
9. Finke C, Freund JA, Rosa E, Braun HA, Feudel U. On the role of subthreshold currents in the Huber–Braun cold receptor model. *Chaos: An Interdisciplinary Journal of Nonlinear Science*. 2010 Dec 30; 20(4). <https://doi.org/10.1063/1.3527989>
10. Olivares E, Salgado S, Maidana JP, Herrera G, Campos M, Madrid R, et al. TRPM8-Dependent Dynamic Response in a Mathematical Model of Cold Thermoreceptor. *Plos One*. 2015 Oct 1; 10(10). <https://doi.org/10.1371/journal.pone.0139314>
11. Voets T, Droogmans G, Wissenbach U, Janssens A, Flockerzi V, Nilius B. The principle of temperature-dependent gating in cold- and heat-sensitive TRP channels. *Nature*. 2004 Aug 12; 430(7001):748–54. <https://doi.org/10.1038/nature02732> PMID: 15306801
12. Hodgkin AL, Huxley AF. A quantitative description of membrane current and its application to conduction and excitation in nerve. *The Journal of physiology*. 1952 Aug 28; 117(4):500–44. <https://doi.org/10.1113/jphysiol.1952.sp004764> PMID: 12991237
13. Mälkiä A, Madrid R, Meseguer V, De La Peña E, Valero M, Belmonte C, et al. Bidirectional shifts of TRPM8 channel gating by temperature and chemical agents modulate the cold sensitivity of

- mammalian thermoreceptors. *The Journal of physiology*. 2007 May 15; 581(1):155–74. <https://doi.org/10.1113/jphysiol.2006.123059> PMID: 17317754
14. Ermentrout B. XPPAUT v 8.00. 2016 Jan. URL <http://www.math.pitt.edu/bard/xpp/xpp.html>.
 15. MATLAB. version 7.10.0 (R2010a). Natick, Massachusetts: The MathWorks Inc.; 2010.
 16. MacDonald DI, Wood JN, Emery EC. Molecular mechanisms of cold pain. *Neurobiology of Pain*. 2020 Jan 1; 7:100044. <https://doi.org/10.1016/j.ynpai.2020.100044> PMID: 32090187